Macromolecules
ARTICLE

Macromolecules **2010**, *43*, 3325–3330 **3325**
DOI: 10.1021/ma100026f

Nanoporous Polyporphyrin as Adsorbent for Hydrogen Storage

Jiangbin Xia,[†] Shengwen Yuan,[‡] Zhuo Wang,[†] Scott Kirklin,[‡] Brian Dorney,[‡] Di-Jia Liu,*[,‡] and Luping Yu*[,†]

[†]*Department of Chemistry and The James Franck Institute, The University of Chicago, 929 E. 57th Street, Chicago, Illinois 60637, and* [‡]*Chemical Sciences & Engineering Division, Argonne National Laboratory, 9700 S. Cass Ave., Argonne, Illinois 60439*

Received January 5, 2010

ABSTRACT: Novel polyporphyrins with high surface area over 1500 m^2/g have been synthesized, and their hydrogen absorption capacities were measured. Porphyrin functionalized with thiophenyl groups was designed as starting monomer; the porphyrin cores offer coordination sites for metal ions which could potentially enhance the interaction with hydrogen for favorable hydrogen storage while the thiophenyl groups are used for cross-linking the monomers under oxidative coupling conditions to yield highly porous networks. These polyporphyrins adsorb up to 5.0 mass % H_2 at 77 K and 65 bar. Compared with metal free polymer, iron(II)-containing polymer shows finite increase in heat of adsorption for hydrogen, suggesting a promising approach for designing high heat of adsorption porous materials.

Introduction

With high conversion efficiency and zero CO_2 emission, hydrogen is considered as an ideal energy carrier in future transportation applications. However, limited on-board capacity of storage media represents one of the major bottlenecks for implementing H_2 as vehicular fuel. Currently, numerous hydrogen storage materials are being developed, including metal/chemical hydrides and sorption-based materials.[1] Distinct from hydride-based adsorbents, sorption-based materials adsorb hydrogen through physisorption without breaking the H−H bond and therefore consume minimum parasitic energy during H_2 extraction. Examples of sorption-based material include metal−organic frameworks (MOFs),[2] engineered carbons,[3] porous polymers,[4] etc. Among them, porous polymers are attractive in their flexibility in structural modification, light weight, and high thermal stability. Although porous polymer does not hold the highest surface area among sorption materials at present, the combination of low skeleton density and high micropore volume makes it more promising to be engineered to meet both gravimetric (1.8 kWh/kg) and volumetric (1.3 kWh/L) capacity targets simultaneously set by U.S. Department of Energy than other candidates, even those with higher surface areas. Different cross-linked porous polymers termed as hyper-cross-linked polymers (HCPs),[4a] polymers of intrinsic microporosity (PIMs),[4b] and covalent organic frameworks (COFs)[4c] have been developed for hydrogen storage. At present, the storage capacity at ambient temperature remains a challenge due to weak interaction between hydrogen and substrate.[1,5]

To improve storage capacity, chemically modified polymeric adsorbents with higher H_2 adsorption energy than the existing polymers are needed. Theoretical calculations as well as experimental results show that metal ions in a porous network could increase the adsorption energy through d−s electronic orbital interaction.[6] A porous polymer framework containing properly designed ligation sites for coordinating and exchanging of transition metal ions could serve as an ideal platform to study metal−hydrogen interaction in a confined space. Metalloporphyrin is an excellent example. With a large number of metal ions could be readily incorporated into the porphyrin center, metalloporphyrin can serve as an exceptional model system for systematic investigation of the impact of metal ion on heat of adsorption if a porphyrin group can be integrated into a high surface area, porous framework. Preparing high surface area porphyrinic metal organic frameworks (MOF), however, turned out to be surprisingly difficult.[7] Porous network polymers based on porphyrin[8a] and phthalocyanine[8b] via dioxane formation reactions yielded Brunauer−Emmett−Teller (BET) surface areas below 1000 m^2/g. Herein, we report our recent effort in preparing two highly porous porphyrinic polymers by covalently cross-linking porphyrin monomers functionalized with thiophenyl groups (Scheme 1). The thiophenyl groups at the branches of the monomer allow oxidative polymerization, and the porphyrin cores provide coordination sites for various metal ions. In addition, the polyporphyrins we prepared yielded narrow pore size distribution and high surface area with BET surface area >1500 m^2/g. Furthermore, they demonstrated an interesting yet desirable positive pressure dependence on hydrogen uptake with capacity larger than 5.0 mass % at 77 K.

*Corresponding authors. E-mail: lupingyu@midway.uchicago.edu (L.Y.), djliu@anl.gov (D.-J.L.).

Results and Discussion

Synthesis of Monomers and Porous Polymers. The designed porphyrin monomer was synthesized as shown in Scheme 1. The 3,5-dibromobenzaldehyde **1** was synthesized according to the literature procedure.[9] The palladium-mediated Stille coupling reaction was used to introduce thiophenyl group to yield compound **2**. The resulting porphyrin monomer was polymerized through oxidative coupling of the terminal thiophenyl groups in anhydrous chloroform using $FeCl_3$ as the oxidant. The polymer containing Fe(II) was obtained by polymerization of corresponding Fe(II)−porphyrin complex.

Structural Characterizations. The structural information was obtained using Fourier transform infrared (FTIR) spectrometer. A comparison of the FTIR spectra of these two polymers and their respective monomers is shown in Figure 1. Two peaks at 3314 and 965 cm^{-1} in the spectrum of

Published on Web 03/05/2010

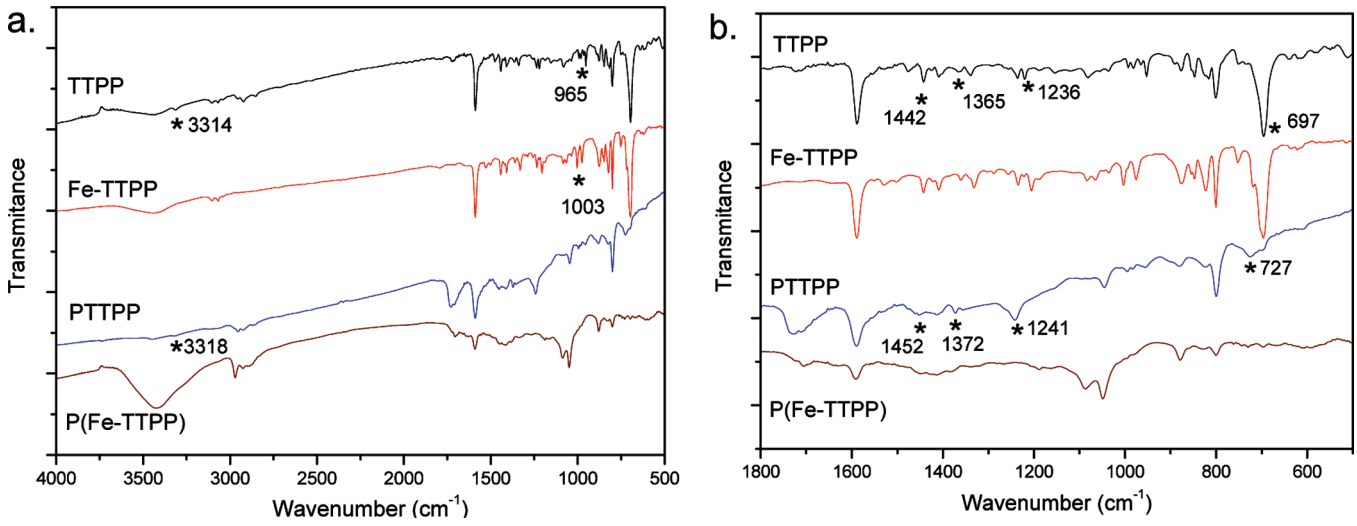

Figure 1. (a) FTIR spectra for the TTPP, Fe-TTPP, and their corresponding polymers. (b) Expansion of (a) for the region from 500 to 1800 cm^{-1}.

Scheme 1. Synthesis of Polymer PTTPP and P(Fe-TTPP)

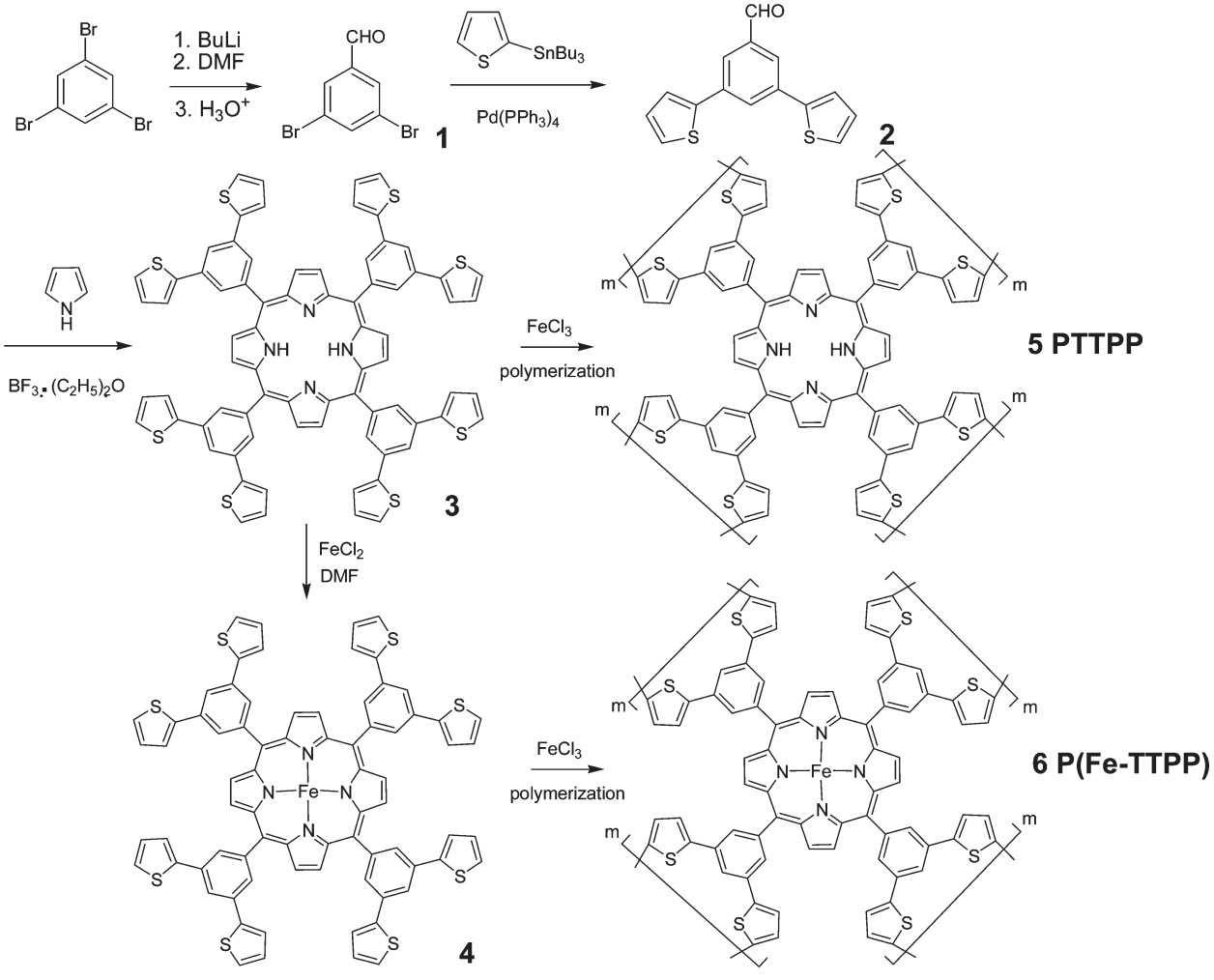

metal free porphyrin (TTPP) are assigned to N−H stretching and in-plane bending vibration of the pyrrole group, respectively.[10] These peaks disappear after forming a Fe−porphyrin complex (Fe-TTPP). It is known that the band at 1000−920 cm^{-1} is metal-sensitive in the porphyrin−metal complex.[11] When Fe(II) ion was inserted into porphyrin ring, a strong sharp peak at 1003 cm^{-1} appeared. In TTPP, peaks at 1442, 1365, and 1236 cm^{-1} originate from the stretching of C=C and C−C in the thiophene ring.[12] After polymerization, these peaks shift to 1452, 1372, and 1241 cm^{-1}, respectively. In addition, the peak intensity at 697 cm^{-1} related to in-plane deformation of C−S−C of thiophene ring decreases

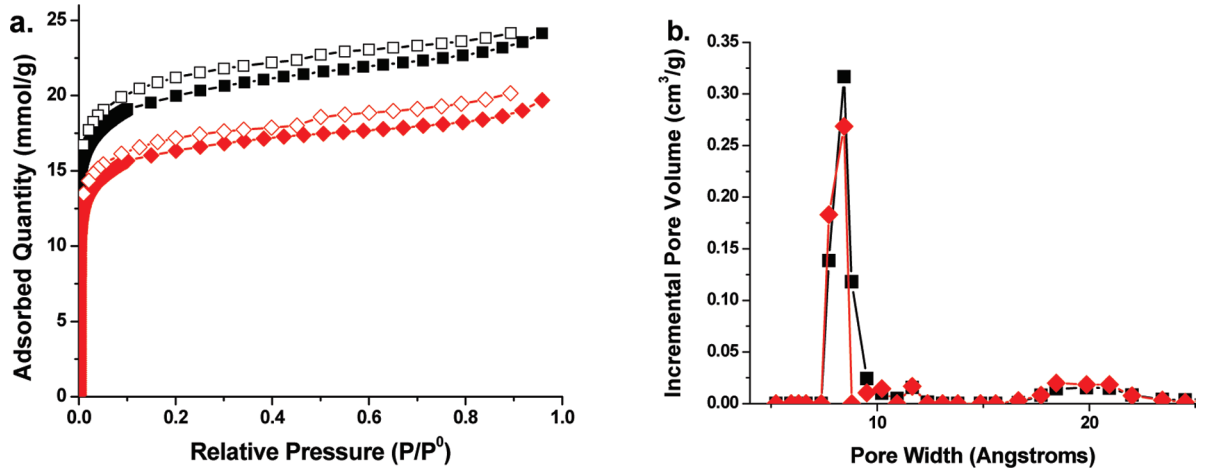

Figure 2. (a) Nitrogen adsorption (filled symbol)/desorption (open symbol) isotherms for polymer PTTPP (square symbol) and P(Fe-TTPP) (diamond symbol). (b) Pore size distribution of polymer PTTPP (square symbol) and P(Fe-TTPP) (diamond symbol), calculated using the NLDFT method.

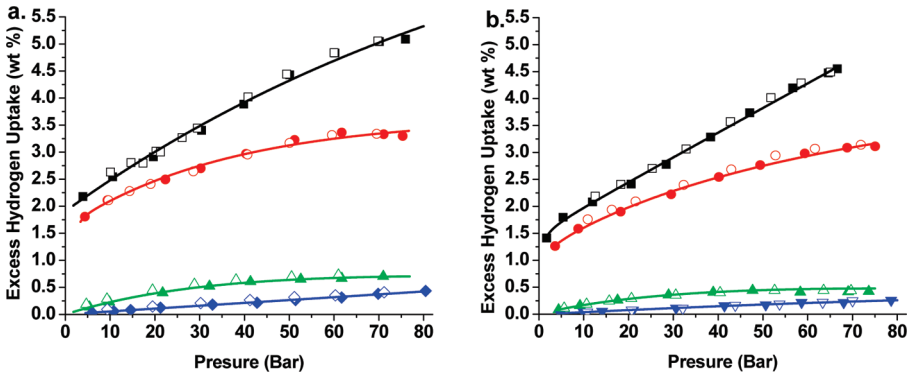

Figure 3. Excess hydrogen adsorption (solid symbols)/desorption (open symbols) isotherms under 77 K (squares), 87 K (circles), 195 K (triangles), and 298 K (diamonds) for polymer PTTPP (a) and polymer P(Fe-TTPP) (b).

Table 1. Surface Properties of PTTPP and P(Fe-TTPP)

	BET surface area (m^2/g)	Langmuir surface area (m^2/g)	total pore volume (cm^3/g)[a]	micropore volume (cm^3/g)[a]	dominant pore diameter (nm)[a]
PTTPP	1522	2030	0.85	0.67	0.85
P(Fe-TTPP)	1248	1665	0.68	0.54	0.82

[a] Data calculated from nitrogen adsorption isotherms with the nonlocal density function theory (NLDFT) method.

while the peak intensity at 727 cm^{-1} (deformation C−S) increases after polymerization.[12]

Porous Polymer Surface Properties. Surface area and pore size distribution were characterized with nitrogen as probing gas at 77 K using a Micromeritics ASAP 2010 system. Both polymers exhibit type I isotherms, as shown in Figure 2a. Figure 2b shows the incremental pore volumes as the function of pore size derived from N_2 adsorption isotherms using a nonlocalized density function theory (NLDFT) method. The majority of the pore volume of these two polymers is contributed from the micropores with narrow pore sizes distribution centered at about 0.8 nm, a desirable dimension for gas adsorption. The introduction of Fe at the center of the porphyrin reduced slightly the dominant pore size and the surface area. Table 1 summarizes the surface properties of the polymers.

Hydrogen Sorption Capacities and Isosteric Heat of Adsorption. Hydrogen adsorption isotherms of the polymers as well as reference adsorbents were measured with a modified Sievert type apparatus.[13] Figure 3 shows the excess H_2 adsorption capacities measured under various equilibrium pressures at four different temperatures. The uptake capacity for polymer PTTPP reaches as high as 5.0 wt % at 77 K and 65 bar, while polymer P(Fe-TTPP) adsorbs up to 4.6 wt % under the same conditions. Interestingly, we observed that the adsorption uptake for both polymers at 77 K showed significant positive pressure dependence up to 60−70 bar, taking up substantially higher amount of hydrogen than what would be predicated by the Chahine's rule (1 wt %/500 m^2/g).[14] This behavior is strikingly different from that of more rigid and open structured adsorbents such as activated carbon or most MOFs which saturates around 10−20 bar at 77 K (see Supporting Information). This suggests that, as pressure increases, H_2 may continually permeate into the "hidden" micropores and surface area in the polymers as the result of conformation change under elevated pressure, possibly due to rotation and stretching of the linking units in the randomly packed network. Such micropores may not be accessible to nitrogen at low pressure during surface area measurement.

The isosteric heat of adsorption at low coverage region was derived from the isotherms measured at 195 and 298 K.

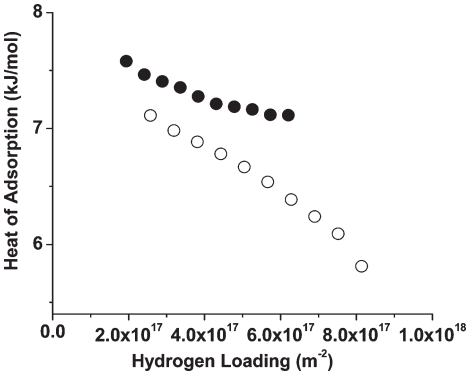

Figure 4. Comparison of heat of adsorption of polymer PTTPP (open circles) and P(Fe-TTPP) (solid circles) at constant hydrogen loading (normalized by surface area).

These two temperatures were chosen because their isotherm plots are well-separated from which the heat of adsorption at initial hydrogen adsorption can be more accurately derived, in contrast to the approach from 77 and 87 K measurements. The heat of adsorption as the function of hydrogen loading is shown in Figure 4. For better comparison between these two polymers with different surface areas, hydrogen loading (*x*-axis) was normalized as the number of H_2 adsorbed per unit surface (m^2). Introducing Fe ions at the porphyrin cores shows a finite effect on increasing the heat of adsorption as indicated by a slightly larger value of P(Fe-TTPP) than that of PTTPP. The limited but definitive increase clearly indicates the modification of interaction of TTPP with H_2 by Fe ions albeit a small magnitude. After the completion of this experimental study, we were brought to attention of a very recent theoretical investigation in which nondissociative interaction of dihydrogen with Fe and other transition metal porphyrins was reported.[15] This study suggested a relatively low H_2 heat of adsorption improvement over Fe−porphyrin (1.9 kJ/mol) unless the symmetry is broken by a substituting ligand. This result appears to agree with our experimental observation of low impact by Fe. The study further indicates that other metals, such as Ti and V, may lead to higher adsorption energy when incorporated into porphyrin. Since our polyporphyrin polymer provides a versatile venue for exchanging metals through coordination chemistry, it can be used for systematic investigation of different transition metal−hydrogen interaction in a confined space which is currently underway in our laboratories.

Conclusion

In summary, two polyporphyrins were synthesized with surface area as high as 1522 m^2/g. Hydrogen uptake of 5 wt % was obtained at 77 K and 65 bar. Furthermore, slight increase in heat of adsorption was observed after insertion of Fe(II) ions into the porphyrin rings. Such system can be used as a platform for doping a wide range of transition metals inside of porous framework in a process of continually improving dihydrogen adsorption energy and capacity.

Experimental Section

Materials. Chemicals were purchased from Aldrich, Alfa Asia, and Strem and were used without further purification unless otherwise noted. *N*,*N*-Dimethylformamide (DMF) anhydrous solvent was distilled from commercial DMF with CaH_2. Pyrrole was distilled before use.

Equipment. ^1H and ^{13}C NMR spectra were collected on a Bruker 400 or 500 MHz FT NMR spectrometer. FTIR spectra were recorded on a Thermo Nicolet Nexus 670 FTIR spectrometer. Thermogravimetric analysis (TGA) data were obtained from a Shimadzu TGA-50 with a heating rate of 10 °C/min in a nitrogen atmosphere. Surface area and porosity were measured using a Micromeritics ASAP 2010 system with nitrogen as probing gas at 77 K. The isotherms of N_2 adsorption/desorption were obtained with high resolution at low pressure region so that detailed information on pore size of the polymers could be extracted. Surface area, pore volumes, and dominant pore size were derived from the N_2 adsorption isotherms using BET and Langmuir models and NLDFT calculation. The hydrogen adsorption isotherms at 77, 87, 195, and 298 K were measured using liquid nitrogen, liquid Ar, dry ice/acetone, and temperature-controlled water as coolant with a modified Sievert isotherm apparatus similar to that reported in the literature.[16] Ultrahigh-purity hydrogen of 99.9995% was used for H_2 update measurement, and free volume of the sample cell at each temperature was calibrated with helium (99.9995%). Hydrogen equilibrium pressure up to 80 bar was applied for the measurement. A typical measurement error was $<\pm 5\%$ of the uptake value obtained at the high-pressure region. The error reduced to $<\pm 2.5\%$ at the low-pressure region. Commercial software, GASPAK, was used to accurately calculate the state equations of hydrogen and helium under different pressures and temperatures. For free volume calibration, helium was dosed to the sample cell in appropriate constant temperature bath, a series values of free volume of the sample cell were calculated at different equilibrium pressure (in the range of 2−50 bar), a linear fit was then applied to these values, and the extrapolated value at zero pressure was used as the free volume for subsequent H_2 uptake calculation.[15] A dual channel high-precision pressure gauge, model CPG 2500 from Mensor with accuracy of 0.01% FS, was installed in the system. The reference section of the isotherm apparatus was encased inside of thermally insulated box with the temperature controlled by circulating water at constant temperature. The sample section was immersed into the liquid bath filled with coolant of different temperature stabilized through phase transition. The liquid level of the coolant was maintained at nearly constant height relative to the sample cell through insulated dewar and constant top-off. In addition, a copper sheath with thermal conduction cross section of 5 cm^2 was attached to the sample cell through liquid/air interphase to compensate any minor variation of liquid level change during the measurement. In our study, typical polymer sample sizes ranged from 200 to 500 mg. Before each isotherm measurement, the sample was weighed after being heat-treated at 125 °C under vacuum to remove residual moisture or other trapped gases. The heat of adsorption was

derived from the slope of ln P vs $1/T$ at constant hydrogen loading using the Clausius−Clapeyron equation:

$$\Delta H = -R\left[\frac{\partial \ln P}{\partial(1/T)}\right]_{n^m} = -Rk \quad (1)$$

where ΔH is the heat of adsorption, R is ideal gas constant, P and T are equilibrium pressure and temperature, respectively, and k is the slop of ln P vs $1/T$ at constant hydrogen loading n^m.[17]

Synthesis of 3,5-Dibromobenzaldehyde (1). Briefly, a suspension of 1,3,5-tribromobenzene (4.0 g, 12.7 mmol) in anhydrous diethyl ether (100 mL) at −78 °C was treated dropwise with butyllithium (5.3 mL, 13.5 mmol). After 45 min dimethylformamide (2.8 g, 38.3 mmol) was added to the mixture, which was then stirred for a further 1 h. Diluted HCl (40 mL, 2 mol/L) was added, then organic phase was removed, and a brown solid was obtained. The crude product was recrystallized from diethyl ether/hexanes to give needles compound **1** (2.4 g, 70%). ^{1}H NMR: δ ($CDCl_3$, ppm): 9.91, s, 1H, CHO, 7.94, (d, J = 1.6 Hz, 2H, Ar−H), 7.92, (t, J = 1.6 Hz, 1H, Ar−H), which is consisted with reported result.[9]

Synthesis of 3,5-Dithiophen-2-yl-benzaldehyde (2). A 100 mL round-bottom flask was charged with 3,5-dibromobenzaldehyde (**1**) (1.81 g, 6.85 mmol), tetrakis(triphenylphosphine)palladium(0) (800 mg, 0.692 mmol), 2-(tributylstannyl)thiophene (6.5 mL, 20.6 mmol), and anhydrous DMF (60 mL) and heated to 80 °C with stirring for 72 h. The reaction mixture was then cooled down to room temperature, diluted with Et_2O, and filtered through Celite. The organic phase was washed with brine and water and dried over $MgSO_4$. After filtration, solvent was removed to yield the crude product which was then chromatographed on silica using a hexane/CH_2Cl_2(2:1) solvent mixture as the eluent. The desired product was a crystalline yellow solid (1.10 g, yield 60%). ^{1}H NMR: δ ($CDCl_3$) 10.09 (1H, s, CHO), 8.06 (1H, t, J = 2.0 Hz, Ar−H), 8.00 (2H, d, J = 2.0 Hz, Ar−H), 7.37−7.15 (6H, m, thiophene-H). ^{13}C NMR: δ ($CDCl_3$) 191.9, 142.5, 137.7, 136.2, 128.8, 128.5, 126.2, 125.8, 124.6. CI-MS: Calcd, 270.4; found $(M + 1)^+$, 271.0. Anal. Calcd for $C_{15}H_{10}S_2$: C, 66.7%; H, 3.70%. Found: C, 67.6%; H, 3.41%.

Synthesis of 5,10,15,20-Tetrakis(3,5-dithiophen-2-ylphenyl)-porphyrin TTPP (3). An oven-dried, three-necked, 1 L, round-bottomed flask equipped with a magnetic stirring bar and a gas-dispersion tube was charged with 3,5-dithiophen-2-yl-benzaldehyde **2** (2.7 g, 0.01 mol), distilled pyrrole (0.7 mL, 0.01 mol), and dichloromethane (600 mL). The solution was purged with nitrogen for 15 min. Boron trifluoride diethyl etherate (0.40 mL, 3.1 mmol) was added via syringe, and the flask was wrapped with aluminum foil to shield it from light. The solution was stirred under a nitrogen atmosphere at room temperature for 1.5 h, and 2,3-dichloro-5,6-dicyano-1,4-benzoquinone (DDQ) (1.7 g, 7.5 mmol) was added directly at one time and keep stirring for another 1.5 h. Then 6 mL of triethylamine was added to neutralize the excessive acid. Then concentrated the solvent and purified with a column. The column was eluted with a mixture of hexane/CH_2Cl_2 (1:1) and offered purple crystal-like solid (0.52 g, 20%). ^{1}H NMR: δ ($CDCl_3$, ppm): 9.04 (s, 8H, pyrrole-H), 8.43 (d, J = 1.6 Hz, 8H, Ar−H), 8.27 (t, J = 1.6 Hz, 4H, Ar−H), 7.57−7.3 (24H, m, thiophene-H), −2.67 (s, 2H). ^{13}C NMR: δ ($CDCl_3$) 143.8, 143.5, 133.7, 131.3, 128.4, 125.7, 124.4, 123.0, 119.6. It is not easy to observe α and β carbon shift in pyrrole ring.[18] UV/vis (λ_{max}, nm $CH_2Cl_2 \times 10^5$ cm^{-1} M^{-1}): 286.5 (1.37), 423.5 (3.54), 516.5 (0.256), 551.5 (0.106), 590.0 (0.091), 646.0 (0.0581). Anal. Calcd for $C_{76}H_{46}N_4S_8$: C, 71.70%; H, 3.61%; N, 4.40%. Found: C, 70.67%; H, 3.51%; N, 4.18%.

Synthesis of Fe-TTPP (4). Fe(II) porphyrin complex was synthesized according to the literature.[19,20] Briefly, porphyrin TTPP (**3**) (0.4 g, 3×10^{-4} mol) was dissolved in 60 cm^3 DMF and $FeCl_2 \cdot 4H_2O$ (0.6 g, 3 mmol) was added to this mixture and boiled for 1 h. The reaction mixture was then cooled down to room temperature and diluted with CH_2Cl_2, and the filtered mixture was washed with brine. The organic phase was collected and dried over $MgSO_4$. After filtration, solvent was removed to yield the crude product which was then chromatographed on silica using a hexane/CH_2Cl_2 (1:1) solvent mixture as the eluent and gave 0.25 g (60%) yield. CI-MS: Calcd, 1325.5; found $(M + 1)^+$, 1326.1. UV/vis (λ_{max}, nm $CH_2Cl_2 \times 10^5$ cm^{-1} M^{-1}) 285.5 (1.16), 416.5 (1.20), 573.0 (0.121), 612.0 (0.07).

Synthesis of PTTPP (5) and P(Fe-TTPP) (6). Anhydrous $FeCl_3$ (0.8 g, 5 mmol) was charged into a round-bottom flask. 10 mL of anhydrous $CHCl_3$ was added and stirred to make a suspension solution. Then a solution of TTPP (0.25 g, 2×10^{-4} mol) or Fe-TTPP (0.26 g, 2×10^{-4} mol) in 20 mL of $CHCl_3$ was added dropwise. The resulting mixture was stirred at room temperature overnight. After that, 200 mL of MeOH was added to the above mixture and kept stirring for another hour. The precipitation was collected by filtration and washed with MeOH. After extraction with CH_2Cl_2, $CHCl_3$, and MeOH/H_2O (volume ratio 1:1) in a Soxhlet extractor for 24 h, the product was dried in vacuum oven at 100 °C overnight. Yield was about 95%.

Hydrogen Isotherm Measurement for Reference Compounds. Two adsorbent materials, AX-21 and Cu-BTC, which are well studied in hydrogen storage application, were used as the references for adsorption isotherm measurement. AX-21 is an engineered active carbon, and Cu-BTC is a metal−organic framework material. Their hydrogen adsorption isotherms are documented in the literature.[21−24] We repeated the hydrogen adsorption of these materials using the identical procedure for the polyporphyrin samples. The excess hydrogen adsorption capacities as the function of pressure are plotted in Figure S7a,b (Supporting Information). These results essentially duplicate that of previously published. Most importantly, they demonstrate saturation or nearly saturation at equilibrium pressure of 20−30 bar, which is strong contrast to that shown in Figure 3 for polymer PTTPP and P(Fe-TTPP).

Acknowledgment. This work was supported by the U.S. Department of Energy's Fuel Cell Technologies program under the Office of Energy Efficiency and Renewable Energy. The authors wish to thank GM and Air Products for providing the AX-21 sample, and thank Ms. Desiree White for experimental support.

Supporting Information Available: Text giving ^{1}H and ^{13}C NMR, UV−vis spectra, and TGA graph of the related compounds; hydrogen adsorption isotherms for an activated carbon AX-21 and a MOF Cu-BTC measured with our modified Sievert apparatus. This material is available free of charge via the Internet at http://pubs.acs.org.

References and Notes

(1) Germain, J.; Fréchet, J. M. J.; Svec, F. *Small* **2009**, *5*, 1098.
(2) (a) Rosi, N. L.; Eckert, J.; Eddaoudi, M.; Vodak, D. T.; Kim, J.; O'Keeffe, M. *Science* **2003**, *300*, 1127. (b) Kaye, S. S.; Long, J. R. *J. Am. Chem. Soc.* **2005**, *127*, 6506.
(3) Liu, C.; Fan, Y. Y.; Liu, M.; Cong, H. T.; Cheng, H. M.; Dresselhaus, M. *Science* **1999**, *286*, 1127.
(4) (a) Lee, J. Y.; Wood, C. D.; Bradshaw, D.; Rosseinsky, M. J.; Cooper, A. I. *Chem. Commun.* **2006**, 2670. (b) McKeown, N. B.; M. Budd, P. *Chem. Soc. Rev.* **2006**, *35*, 675. (c) El-Kaderi, H. M.; Hunt, J. R.; Mendoza-Cortés, J. L.; Côté, A. P.; Taylor, R. E.; O'Keeffe, M.; Yaghi, O. M. *Science* **2007**, *316*, 268.
(5) Zhao, D.; Yuan, D.; Zhou, H. *Energy Environ. Sci.* **2008**, *1*, 222.
(6) (a) Rrr Lochan, R. C.; Head-Gordon, M. *Phys. Chem. Chem. Phys.* **2006**, *8*, 1357. (b) Dinca, M.; Dailly, A.; Liu, Y.; Brown, C. M.; Neumann, D. A.; Long, J. R. *J. Am. Chem. Soc.* **2006**, *128*, 16876.
(7) (a) Shultz, A. M.; Farha, O. K.; Hupp, J. T.; Nguyen, S. T. *J. Am. Chem. Soc.* **2009**, *131*, 4204. (b) Ohmura, T.; Usuki, A.; Fukumori, K.; Ohta, T.; Ito, M.; Tatsumi, K. *Inorg. Chem.* **2006**, *45*, 7988–7990.
(8) (a) McKeown, N. B.; Makhseed, S.; Budd, P. M. *Chem. Commun.* **2002**, 2780. (b) McKeown, N. B.; Hanif, S.; Msayib, K.; Tattershall, C. E.; Budd, P. M. *Chem. Commun.* **2002**, 2782.

(9) Deb, S. K.; Maddux, T. M.; Yu, L. *J. Am. Chem. Soc.* **1997**, *119*, 9079.
(10) Ogoshi, H.; Saito, Y.; Nakamoto, K. *J. Chem. Phys.* **1972**, *57*, 4194.
(11) Ueno, K.; Martell, A. E. *J. Phys. Chem.* **1956**, *60*, 934.
(12) (a) Kvarnström, C.; Neugebauer, H.; Blomquist, S.; Ahonen, H. J.; Kankare, J.; Ivaska, A. *Electrochim. Acta* **1999**, *44*, 2739. (b) Louarn, G.; Kruszka, J.; Lefrant, S.; Zagorska, M.; Kulszewicz-Bayer, I.; Proń, A. *Synth. Met.* **1993**, *61*, 233.
(13) Yuan, S.; Kirklin, S.; Dorney, B.; Liu, D.; Yu, L. *Macromolecules* **2009**, *42*, 1554.
(14) Benard, P.; Chahine, R. *Int. J. Hydrogen Energy* **2001**, *26*, 849.
(15) Kim, Y.-H.; Sun, Y. Y.; Choi, W. I.; Kang, J.; Zhang, S. B. *Phys. Chem. Chem. Phys.* **2009**, *11*, 11400.
(16) Gross, K. J.; Carrington, K. R. DOE: Recommended Best Practices for the Characterization of Storage Properties of Hydrogen Storage Materials (V31, Dec 12, **2008**).
(17) Zhou, W.; Wu, H.; Hartman, M. R.; Yildirim, T. *J. Phys. Chem. C* **2007**, *111*, 16131.
(18) Kozlowski, P. M.; Wolinski, K.; Ye, P. P.; Li, X.-Y. *J. Phys. Chem. A* **1999**, *103*, 420.
(19) Hayvalí, M.; Gündüz, H.; Gündüz, N.; Kílíç, Z.; Hökelek, T. *J. Mol. Struct.* **2000**, *525*, 215.
(20) Adler, A. D.; Longo, F. R.; Kampas, F.; Kim, J. *J. Inorg. Nucl. Chem.* **1970**, *32*, 2443.
(21) Zhou, L.; Zhou, Y.; Sun, Y. *Int. J. Hydrogen Energy* **2004**, *29*, 319.
(22) Ma, S.; Eckert, J.; Forster, P.; Yoon, J.; Hwang, Y. K.; Chang, J.-S.; Collier, C. D.; Parise, J. B.; Zhou, H.-C. *J. Am. Chem. Soc.* **2008**, *130*, 15896.
(23) Wong-Foy, A. G.; Matzger, A. J.; Yaghi, O. M. *J. Am. Chem. Soc.* **2006**, *128*, 3494.
(24) Panella, B.; Hirscher, M.; Pütter, H.; Müller, U. *Adv. Funct. Mater.* **2006**, *16*, 520.